# Kinetic energy distributions and signature of target excitation in $N_2$ fragmentation on collisions with $Ar^{9+}$ ions

Jyoti Rajput,[1,*] Sankar De,[2] A. Roy,[1] and C. P. Safvan[1]
[1]*Inter-University Accelerator Centre, Aruna Asaf Ali Marg, New Delhi 110067, India*
[2]*Department of Physics, University of Calcutta, 92, Acharya Prafulla Chandra Road, Kolkata 700009, India*
(Received 29 May 2006; published 1 September 2006)

The multiple ionization and fragmentation of $N_2$ induced by ion impact is studied using time- and position-sensitive detectors in multihit coincidence mode. With $Ar^{9+}$ at a projectile velocity of 1 a.u., we observe a total of seven fragmentation channels originating from multiply charged transient molecular ions. The preference of symmetric charge breakup channels over the asymmetric ones is clearly observed. A signature of core excitation of the target followed by Auger emission is observed in the $N^{3+}$-$N^{3+}$ fragmentation channel. The kinetic energy release spectra of all the observed fragmentation pathways is explained on the basis of calculated *ab initio* (using the multiconfiguration self-consistent-field method) potential-energy curves.

DOI: 10.1103/PhysRevA.74.032701 PACS number(s): 34.50.Gb, 31.15.Ar, 32.80.Hd

## I. INTRODUCTION

The dynamics of formation and subsequent decay of unstable molecular ions produced due to interaction of neutral molecules with strong potential fields of slow highly charged ions (HCI) is important not only for the fundamental understanding of atomic collision physics but also for practical applications in astrophysics and plasma physics. Molecular fragmentation can be induced by electron impact [1], synchrotron radiation [2], femtosecond lasers [3], as well as multicharged ions [4–7].

The difference between photon-induced and ion-induced dissociation is the interaction time. With the present photon sources (lasers and synchrotron radiation), the interaction times leading to fragmentation are typically of the order of intrinsic molecular vibration and rotation times (10 fs–10 ps), so that the photon field is intertwined with the dissociation process. For slow ions, the interaction times are in the sub-femtosecond regime. Slow multicharged ions because of their large cross section for electron capture are effective sources for studying dissociative ionization.

Multiple ionization of stable molecular systems leads to the formation of unstable or metastable states of the transient molecular ions. An unstable molecular ion dissociates releasing energy in the form of kinetic energy of the dissociated fragments. The metastable states can also decay via tunneling through the potential barrier releasing energy. With the interaction times much smaller than the typical vibrational and rotational time scales of molecules, the molecular excitation is a Frank-Condon process and the kinetic energy release (KER) depends on the internuclear distance at the time of excitation. A distribution of kinetic energies of the fragments is usually observed due to excitation in more than one state of the intermediate molecular ion. Experiments in which the detection of correlated fragment ions is carried out provide valuable information about the charge-state and potential energy surfaces of the multiply charged molecular ions and also shed light on the excitation and fragmentation dynamics.

From the studies on molecular dissociation it is known that in the case of fast collisions in the strong interaction regime (i.e., $Q > v \gg v_0$, where $Q$ is the projectile charge, $v$ its velocity, and $v_0$ the Bohr velocity, all quantities in atomic units), the KER distributions are practically independent of the projectile charge and velocity [8,9], while in the case of low velocity projectiles the shape of the KER spectrum shows a distinct dependence on projectile energy and projectile type [4–6]. In collisions with fast projectiles, direct ionization is the dominant process of electron removal, in contrast to the case of low-energy projectiles where electron capture and transfer ionization are the dominant processes. Ion-induced molecular fragmentation at different energy regimes has shown that electron removal due to capture process transfers less excitation to the target than direct ionization [10]. For studies in which the HCI-molecule interaction times are of the same order as the time scales for molecular dissociation, the subtle effects of the high field of the outgoing projectile are also observed [11,12]. Hence the different energy regimes give information about different excited electronic states of the same multiply charged molecular ion.

Studies on core excitation using soft x rays followed by Auger emission and fragmentation exist in the literature [13–17]. In the sub-keV region, where the 1*s* binding energies of the first-row elements are found, the Auger yield is typically around 99.9%, leaving 0.1% for radiative decay [17]. In the case of electron-ion and ion-ion studies, $CS_2$ upon core electron excitation [18], corresponding to the removal of electrons from the deep valence levels, results in the atomization of the system. The process of Auger deexcitation following direct ionization was reported in electron impact ionization of $H_2O$ [1] and also in the collision of $H^+$ (4–23 keV) with $H_2O$ [19].

In the present paper, we discuss the various dissociation channels of the $N_2^{q+}$ molecular ion, formed during the impact of low-energy $Ar^{9+}$ ($v=v_0$, $v_0$ being the Bohr velocity) on $N_2$. At this projectile velocity, the interaction time of 145 attoseconds is much less than typical rotational and vibrational time periods of the molecule. Hence the molecular core remains essentially frozen during the interaction. This time being much less than the characteristic fragmentation

*Electronic address: jyoti@iuac.res.in

 

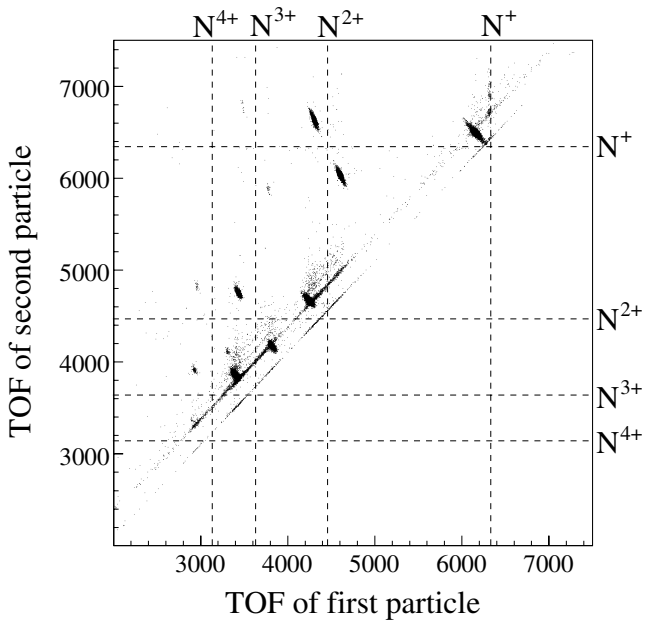


FIG. 1. Coincidence map of the $N_2$ fragmentation.

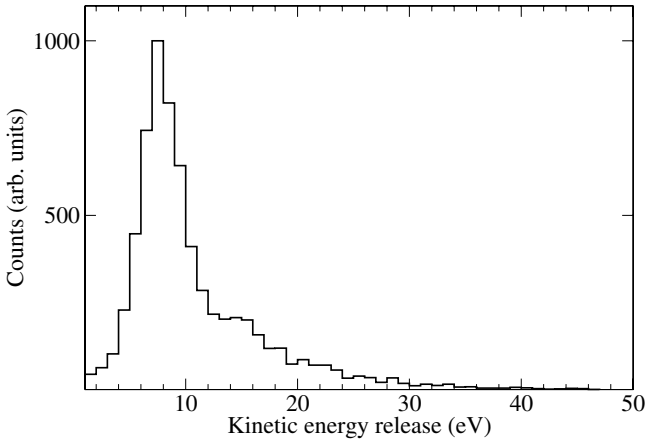


FIG. 2. Kinetic energy release spectra of the $N^+$-$N^+$ fragmentation channel.

times of molecules (around 10 fs [8]), the kinetic energy distribution of the fragments directly reflects the properties of the molecular states of the multiply ionized molecule. We have determined the KER distributions for all seven fragmentation pathways and have calculated *ab initio* potential-energy curves for the $N_2^{q+}$ $(3 \leqslant q \leqslant 6)$ molecular ions to investigate the origin of the kinetic energy releases observed. At the projectile velocity of 1 a.u., transfer ionization is the dominant mode of electron transfer [20]. In transfer ionization, either the projectile, target, or both may be left in excited states during the ion-atom or ion-molecule interaction. The excited particle then relaxes to the ground state via Auger emission or by emitting one or more photons. The process of Auger emission following core excitation is observed in one of the seven fragmentation channels observed in the present experiment and is discussed in light of target excitation. To the best of our knowledge, there is no prior report on the role of target excitation in ion-induced $N_2$ fragmentation.

## II. EXPERIMENT AND DATA ANALYSIS

The experiment was carried out at the Low Energy Ion Beam Facility (LEIBF) of the Inter-University Accelerator Centre (IUAC), New Delhi, India. Low-energy $Ar^{9+}$ ions are produced from a 10 GHz Nanogan ECR ion source placed on a 200 kV high-voltage platform along with its extraction system [21]. The ions are mass analyzed by a 90° bending magnet and transported to the collision chamber at the center of which the projectile ions interact with $N_2$ molecules effusing from a grounded needle located at right angles to the beam direction. The contamination of other charge states in the $Ar^{9+}$ beam was measured to be less than 1%. The dissociated fragments are extracted from the interaction zone in a linear two-field time-of-flight mass spectrometer (TOFMS) by applying a uniform electric field perpendicular to both the ion beam and the gas jet. At the end of the TOFMS, the dissociation products are detected by a position-sensitive microchannel plate (MCP) detector. The ejected electrons are extracted in the opposite direction to TOFMS and detected by a channel electron multiplier that gives the trigger for starting the data acquisition. The TOF spectrum was acquired in multihit mode by a time-to-digital converter (TDC) interfaced to a computer where the fragment ions were recorded in coincidence to obtain information on correlated dissociation products. The details of the setup and data acquisition have been published elsewhere [22].

We have done an event-by-event analysis of the acquired multihit coincidence data to determine the three velocity components and hence the kinetic energy $(\sqrt{v_x^2+v_y^2+v_z^2})$ of each fragment ion individually. The KER distribution was then obtained from the contributions of correlated fragment ion pairs. The velocity component parallel to the TOFMS axis $(v_z)$ is deduced from the measured TOF of the fragment ion. A reference time $t_0$ for each possible fragment ion was calculated from the calibration of the undissociated molecular peaks appearing in the TOF spectrum. The time difference between the measured and the reference values was used along with the TOFMS parameters (i.e., geometry and fields) to determine $v_z$,

$$v_z = \frac{qE(t-t_0)}{m},$$

where $q$ is the charge state of the ion and $E$ is the extraction field of the TOFMS.

The other two components of the velocity ($v_x$ and $v_y$) were determined from the position of impact ($x$ and $y$) of the fragment ion on the MCP. The reference points $x_0$ and $y_0$ were determined for each event by taking the center of mass of the $x$ and $y$ position of each pair of fragments detected in coincidence. The $x$ and $y$ components of the velocity were then determined as

$$v_x = \frac{x-x_0}{t} \quad \text{and} \quad v_y = \frac{y-y_0}{t},$$

where $t$ is the measured TOF of the fragment ion.

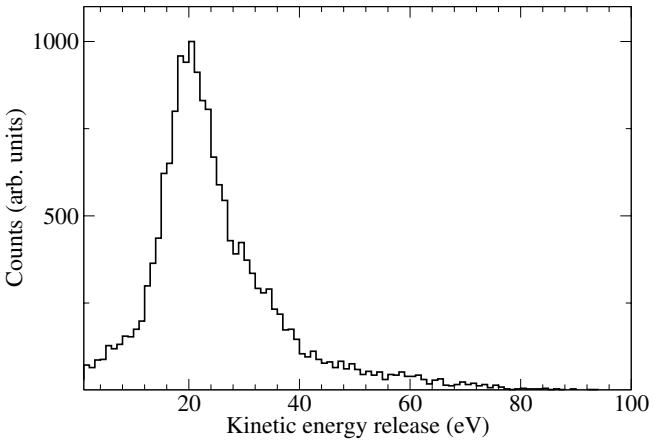


FIG. 3. Kinetic energy release spectra of the $N^+$-$N^{2+}$ fragmentation channel.

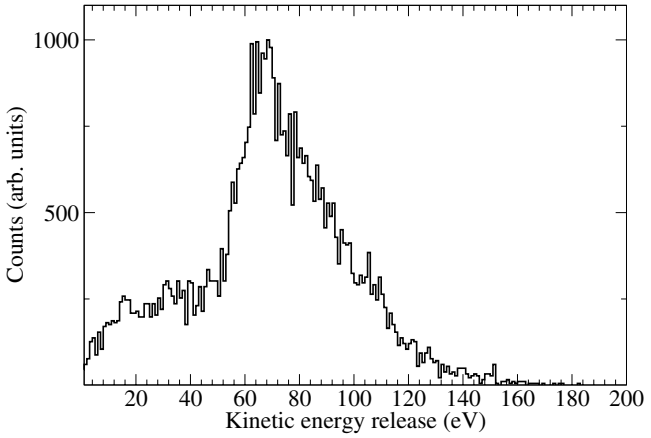


FIG. 5. Kinetic energy release spectra of the $N^{2+}$-$N^{3+}$ fragmentation channel.

## III. RESULTS

Figure 1 shows the coincidence map of the dissociation of $N_2$ following $Ar^{9+}$ impact. From the coincidence map, the interparticle correlations between the different fragment charge states can be clearly identified. Each point in the map is due to the coincident detection of two nitrogen ions originating from the dissociation of the $N_2^{q+}$ molecular ion. The dark patches are due to the high density of points representing the various fragmentation pathways. In a majority of the fragmentation channels, the number of counts obtained is reasonably large except for the two fragmentation channels $N^{3+}$-$N^{1+}$ and $N^{4+}$-$N^{2+}$, where statistics are low. However, in spite of the low statistics, the major energy components in the above-mentioned KER distributions can be considered as we have eliminated the contributions from the overlap of the $N^{3+}$ forward and $N^{4+}$ backward peaks.

Figures 2–6 show the KER distributions for the dissociation channels observed in this experiment. Almost all the KER spectra obtained in the present experiment exhibit a high-energy tail beyond the peak of the KER distribution. Table I lists the most probable KER values for the different fragmentation channels obtained in the present experiment along with the KER values from other experiments studying $N_2$ fragmentation. The values calculated from the pure Coulomb explosion model (see discussion) are also listed.

It should be noted that for the $N_2^{q+}$ molecular ion dissociating into $N^{m+}$-$N^{n+}$, for the ones with even $q$ we observe dissociations with $m=n$ (the symmetric charge breakup channel) and also $m=n+2$ (the asymmetric charge breakup channel). In the case of odd $q$ values, we observe channels with $m=n+1$ only.

To investigate the peaks of the KER spectra, we have calculated *ab initio* potential-energy curves for some of the low-lying states of $N_2^{q+}$ $(3 \leqslant q \leqslant 6)$ molecular ions. The MCSCF energies are calculated as a function of the internuclear distance for $N_2^{q+}$ $(3 \leqslant q \leqslant 5)$ with a 6-311G basis set including three $d$-type and one $f$-type polarization functions using the GAMESS [23] package. For the $N_2^{6+}$ molecular ion, we did a UHF calculation using the same basis set. Using the MCSCF method, we have also calculated the various asymptotic limits for the decay of the transient molecular ions. Our values for the excitation energy of the atomic ions are in good agreement with the NIST database values [24]. Our calculated value for the excitation of $N^+(^3P)$ to $N^+(^1D)$ is 2.0 eV (1.9 eV), for $N^{2+}(^2P)$ to $N^{2+}(^4P)$ is 6.99 eV

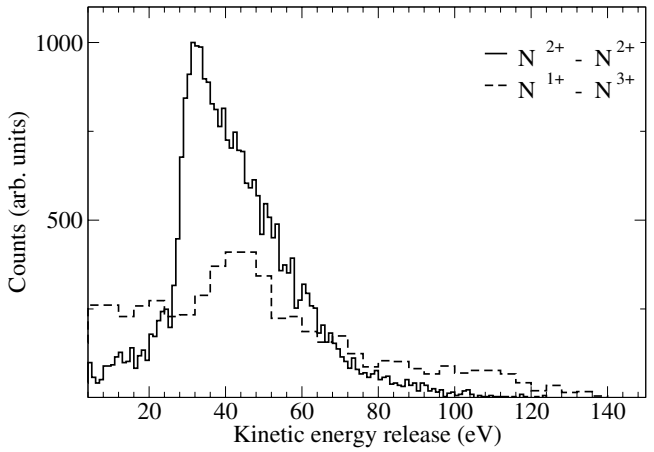


FIG. 4. Kinetic energy release spectra of the $N^{2+}$-$N^{2+}$ and $N^{1+}$-$N^{3+}$ fragmentation channel.

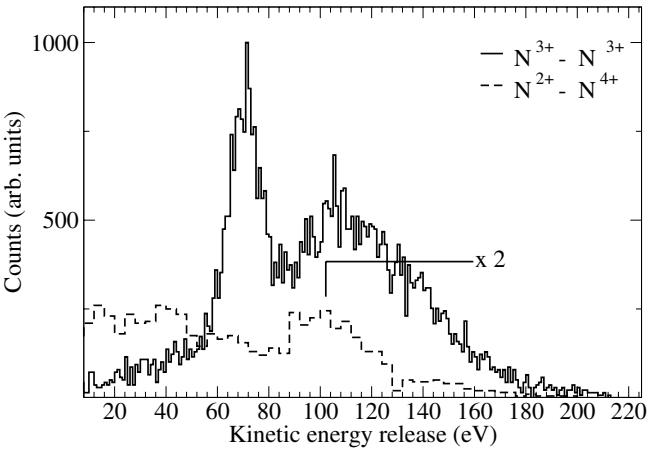


FIG. 6. Kinetic energy release spectra of the $N^{3+}$-$N^{3+}$ and $N^{2+}$-$N^{4+}$ fragmentation channel.

TABLE I. This table shows the KER values obtained for the various fragmentation channels $N^{r+}$-$N^{s+}$ in $N_2$ fragmentation induced by ion impact. The values calculated from the pure Coulomb explosion model are also included.

| Fragmentation channel | KER values (eV) for different projectile velocities | | | Coulomb energies (eV)[a] |
|---|---|---|---|---|
| | 5.9 MeV/amu [8] | 0.2 keV/amu [31] | 24 keV/amu (this work) | |
| $N^{1+}$-$N^{1+}$ | 14.5 | 10.6 | 7.5, 14.5 | 13.1 |
| $N^{1+}$-$N^{2+}$ | 30.3 | 22.2 | 20 | 26.2 |
| $N^{1+}$-$N^{3+}$ | 53.5 | | 20, 44 | 39.3 |
| $N^{2+}$-$N^{2+}$ | 51.3 | 39.0 | 32.5 | 52.5 |
| $N^{2+}$-$N^{3+}$ | 79.9 | 72.2 | 68 | 78.7 |
| $N^{2+}$-$N^{4+}$ | 103.2 | | 40, 100 | 104.9 |
| $N^{3+}$-$N^{3+}$ | 108.7 | 112.6 | 72, 105 | 118.0 |

[a]At equilibrium internuclear distance of 1.089 Å.

(7.09 eV), and for $N^{3+}(^1S)$ to $N^{3+}(^3P)$ is 8.32 eV (8.33 eV), which agrees well with the NIST values (given in parentheses). Table II shows the results of our calculations in terms of KERs when the various states of the $N_2^{q+}$ $(3 \leqslant q \leqslant 6)$ molecular ion decay into two atomic fragments in their lowest possible states. Thus the tabulated values of the KER denote the upper limit of the KER in each fragmentation channel. We now discuss each of the fragmentation channels individually.

### A. Decay of $N_2^{2+}$

The KER spectrum corresponding to the $N^+$-$N^+$ fragmentation channel (Fig. 2) shows two major energy components, one at 7.5 eV and another at 14.5 eV. Table III lists the various molecular states of $N_2^{2+}$ (taken from [25]) and the associated energy release, when they dissociate into two $N^+$ ions in their $^3P$ ground state. Many of these states are metastable in their lowest vibrational levels with very long tunneling lifetimes. In the present experiment, only the higher vibrational levels of these states are excited by a vertical Frank-Condon transition and undergo dissociation releasing energy. The theoretical energy release values are in good agreement with the experimentally obtained KER values. In electron impact ionization experiments [26], similar energy releases have been observed for $N_2^{2+}$ decay. The higher resolution in those experiments enables the separation of the individual vibrational levels leading to dissociation into the $N^+$-$N^+$ ion pair. In the present experiment, excitation into the low-lying $a\ ^3\Pi_u$ and $A\ ^1\Pi_u$ states of $N_2^{2+}$ has not been observed.

TABLE II. Theoretically calculated values of KER in the case of $N_2^{q+}$ $(3 \leqslant q \leqslant 6)$ dissociating to the lowest possible states of $N^{m+}+N^{n+}$ with $m+n=q$. These values denote the upper limit of the KER.

| Dissociation channels | Kinetic energy release (eV) |
|---|---|
| $N_2^{3+}(^2\Sigma) \rightarrow N^{2+}(^2P)+N^{1+}(^3P)$ | 25.40 |
| $N_2^{3+}(^4\Sigma) \rightarrow N^{2+}(^2P)+N^{1+}(^3P)$ | 19.77 |
| $N_2^{4+}(a\ ^5\Sigma) \rightarrow N^{2+}(^2P)+N^{2+}(^4P)$ | 35.48 |
| $N_2^{4+}(a\ ^5\Sigma) \rightarrow N^{1+}(^3P)+N^{3+}(^3P)$ | 33.07 |
| $N_2^{4+}(b\ ^5\Sigma) \rightarrow N^{2+}(^2P)+N^{2+}(^4P)$ | 45.40 |
| $N_2^{4+}(b\ ^5\Sigma) \rightarrow N^{1+}(^3P)+N^{3+}(^3P)$ | 42.89 |
| $N_2^{4+}(^3\Sigma) \rightarrow N^{2+}(^2P)+N^{2+}(^2P)$ | 46.59 |
| $N_2^{4+}(^3\Sigma) \rightarrow N^{1+}(^3P)+N^{3+}(^1S)$ | 28.78 |
| $N_2^{5+}(^2\Sigma) \rightarrow N^{2+}(^2P)+N^{3+}(^1S)$ | 67.56 |
| $N_2^{5+}(^4\Sigma) \rightarrow N^{2+}(^4P)+N^{3+}(^1S)$ | 59.68 |
| $N_2^{6+}(^1\Sigma) \rightarrow N^{3+}(^1S)+N^{3+}(^1S)$ | 114.67 |
| $N_2^{6+}(^1\Sigma) \rightarrow N^{2+}(^2P)+N^{4+}(^2S)$ | 86.96 |
| $N_2^{6+}(^3\Sigma) \rightarrow N^{3+}(^1S)+N^{3+}(^3P)$ | 98.46 |
| $N_2^{6+}(^3\Sigma) \rightarrow N^{2+}(^4P)+N^{4+}(^2S)$ | 69.80 |

### B. Decay of $N_2^{3+}$

The maximum KER that can be released on dissociation of $N_2^{3+}$ is 25.40 eV. The peak of the KER spectra of the $N^+$-$N^{2+}$ fragmentation channel (Fig. 3) occurs at around 20 eV and can be explained by considering the decay of $N_2^{3+}$ to $N^{2+}$ $(^2P)$, the ground state of $N^{2+}$ and $N^{1+}$ $(^1S)$, and the excited state of $N^{1+}$,

$$N_2^{3+}(^2\Sigma) \rightarrow N^{2+}(^2P) + N^{1+}(^1S),\ 21.35\ \text{eV}.$$

The high-energy components of the KER spectra are possibly coming from the dissociation of the higher excited states

TABLE III. The possible molecular states of $N_2^{2+}$ dissociating into $N^+(^3P)+N^+(^3P)$ along with the theoretically calculated values of KER [25].

| Molecular states | Release energy (eV) |
|---|---|
| $d\ ^1\Sigma_g^+$ | 8.4 |
| $c\ ^1\Delta_g$ | 8.1 |
| $D\ ^3\Pi_g$ | 7.9 |
| $g\ ^1\Sigma_g^+$ | 14.2 |
| $h\ ^1\Sigma_u^-$ | 14.9 |
| $G\ ^3\Pi_g$ | 15.2 |
| $B\ ^3\Sigma_u^-$ | 14.1 |

of $N_2^{3+}$. Our values for the lowest electronic state of the $N_2^{3+}$ molecular ion are in agreement with the calculations given in Ref. [27], and the high-energy component of our KER spectra can be explained on the basis of the higher excited states of $N_2^{3+}$ calculated in the same reference.

### C. Decay of $N_2^{4+}$

The $N_2^{4+}$ molecular ion can dissociate to give either $N^{2+}$-$N^{2+}$ (the symmetric channel) or $N^{+}$-$N^{3+}$ (the asymmetric channel) (Fig. 4). The dominant channel observed is the symmetric one. Our calculations for the lowest states of $N_2^{4+}$ explain the KER spectrum of the $N^{2+}$-$N^{2+}$ and $N^{+}$-$N^{3+}$ fragmentation channels. In the cases in which the KER value is lower than the maximum KER (Table II), the decay to excited states of the atomic fragments explains the experimentally observed values,

$$N_2^{4+}(b^5\Sigma) \rightarrow N^{2+}(^2D) + N^{2+}(^4P),\ 32.88\ \text{eV},$$

$$N_2^{4+}(a^5\Sigma) \rightarrow N^{1+}(^3D) + N^{3+}(^3P),\ 21.64\ \text{eV},$$

$$N_2^{4+}(b^5\Sigma) \rightarrow N^{1+}(^3P) + N^{3+}(^3P),\ 42.89\ \text{eV}.$$

In the Frank-Condon region, the $a\ ^5\Sigma$ state is the ground state of the $N_2^{4+}$ molecular ion. It cannot dissociate into two $N^{2+}$ ions in their $^2P$ ground states because of the spin conservation rules. It can, however, decay into one ground state $N^{2+}(^2P)$ and one excited $N^{2+}(^4P)$ ion with the release of 35.48 eV as KER. The most probable energy of 32.5 eV obtained in our experiment is lower than this by about 5 eV, which can result if $b\ ^5\Sigma$ decays into two excited states of $N^{2+}$, namely the $(^4P)$ and the $(^2D)$ state.

The KER spectra for the $N^{+}$-$N^{3+}$ channel shows two energy components. The lower-energy component around 20 eV can come from the decay of $a\ ^5\Sigma$ into $N^{1+}(^3D) + N^{3+}(^3P)$ releasing around 21.64 eV. The origin of the high-energy component (44 eV) is the decay of $b\ ^5\Sigma$ into $N^{1+}(^3P) + N^{3+}(^3P)$ releasing around 42.89 eV energy.

### D. Decay of $N_2^{5+}$

The fragmentation channel of $N^{2+}$-$N^{3+}$ (Fig. 5) has its origin in the dissociation of the $N_2^{5+}$ molecular ion. The most probable KER value in this case is around 68 eV. From our calculated potential-energy curve for $N_2^{5+}$ we find that the dissociation of the $^2\Sigma$ ground state of this ion into two ground-state ions of $N^{2+}(^2P)$ and $N^{3+}(^1S)$ explains the most probable KER,

$$N_2^{5+}(^2\Sigma) \rightarrow N^{2+}(^2P) + N^{3+}(^1S),\ 67.56\ \text{eV}.$$

### E. Decay of $N_2^{6+}$

In this case, as for $N_2^{4+}$, we find that the symmetric channel dominates the fragmentation products. The high-energy peak in the KER spectra of the $N^{3+}$-$N^{3+}$ channel (Fig. 6) at around 105 eV can be explained from our UHF calculations on the $N_2^{6+}$ molecular ion,

$$N_2^{6+}(^1\Sigma) \rightarrow N^{3+}(^1S) + N^{3+}(^1S),\ 114.7\ \text{eV}.$$

Our UHF calculations are in reasonable agreement with the experimentally obtained value. Although we cannot identify the most probable KER value for the $N^{2+}$-$N^{4+}$ fragmentation channel due to poor statistics, two distinct energy components are clearly visible in the KER spectrum. The low-energy component (40 eV) in this channel can be explained from the decay of the transient $^3\Sigma$ state of the molecular $N_2^{6+}$ ion decaying into ground as well as excited states of the atomic fragments. The high-energy component above 100 eV cannot be explained from the low-lying $^1\Sigma$ and $^3\Sigma$ states of $N_2^{6+}$. This component is possibly coming from the higher excited states of the $N_2^{6+}$ molecular ion,

$$N_2^{6+}(^3\Sigma) \rightarrow N^{2+}(^2P) + N^{4+}(^2S),\ 86.96\ \text{eV},$$

$$N_2^{6+}(^3\Sigma) \rightarrow N^{2+}(^4P) + N^{4+}(^2S),\ 69.8\ \text{eV},$$

$$N_2^{6+}(^3\Sigma) \rightarrow N^{2+}(^2P) + N^{4+}(^4P),\ 35.4\ \text{eV},$$

$$N_2^{6+}(^3\Sigma) \rightarrow N^{2+}(^4P) + N^{4+}(^4P),\ 28.3\ \text{eV},$$

$$N_2^{6+}(^3\Sigma) \rightarrow N^{2+}(^2D) + N^{4+}(^4P),\ 22.9\ \text{eV}.$$

The low-energy sharp peak at around 72 eV in the $N^{3+}$-$N^{3+}$ fragmentation channel cannot be explained by molecular dissociation of $N_2^{6+}$. This energy is very close to the most probable KER in the case of $N_2^{5+}$ fragmentation (68 eV). The difference of around 4 eV in the most probable KER obtained in the case of $N^{2+}$-$N^{3+}$ fragmentation channel and the low-energy peak in the $N^{3+}$-$N^{3+}$ KER spectra can be explained by the population of highly excited states of the $N_2^{5+}$ transient molecular ion dissociating into $N^{2+}$-$N^{3+}$. The origin of this energy component thus lies in the Auger decay of the $N^{2+}$ ion formed from the dissociation of highly excited states of $N_2^{5+}$ into $N^{2+}$ and $N^{3+}$.

## IV. DISCUSSION

Experimental measurements of the KER's have shown that the energy releases are usually lower than those predicted by the Coulomb explosion model [$E(\text{eV}) = 14.4 q_1 q_2 / R\ (\text{Å})$, where $q_1$ and $q_2$ are the charges on the two fragments and $R$ is the internuclear distance of the neutral parent molecule]. In the Coulomb explosion model, the simplest model describing a breakup of molecular ions, a point charge is put on each atom of a molecular ion and the motion of each atom is governed by the Coulomb repulsion from the others. Since the Coulomb explosion model does not take into account the electronic charge cloud in the internuclear region, generally it predicts a higher KER than that obtained experimentally. In a simple Coulombic model, the width of the KER distribution is determined by the reflection of the ground-state probability density off the Coulomb potential curve [28]. The resulting KER distribution is approximately a Gaussian with a width of a few eV [29,30], which is much less than the observed width of up to 120–140 eV for higher degrees of ionization in the present

experiment. Hence the Coulomb explosion model is insufficient to explain either the most probable KER or the observed width of the KER spectra.

If the fragmented atomic ions are left in an excited state upon molecular dissociation, the resultant KER would be lower than that expected with the fragment ions in their respective ground states. On the other hand, excited transient molecular ions dissociating into ground-state atomic fragments would result in a higher KER as compared to that obtained on dissociation of ground-state molecular ions. The high-energy component observed in almost all the KER spectra thus hints toward the contribution of excited molecular states to the KER spectra.

Experiments studying $N_2$ dissociation at high impact energies [8] have yielded higher values of KER than those obtained in the present experiment. This may be because at high projectile energies, higher excited states of $N_2^{q+}$ molecular ions are populated, leading to larger KER values on dissociation.

Remscheid *et al.* [31] have calculated potential-energy curves for $N_2^{4+}$ and $N_2^{6+}$ molecular ions to explain their study on $N_2$ fragmentation induced by an $Ar^{8+}$ (8 keV) projectile. They have concentrated on the symmetric channel of charge breakup of $N_2^{4+}$ and $N_2^{6+}$. In our experiment, we observe both the symmetric and the asymmetric charge breakup of the $N_2^{4+}$ and $N_2^{6+}$ so we have calculated the potential-energy curves for these molecular ions to investigate the origin of the energy peaks in our KER spectra. For the symmetric breakup, our theoretical values are in agreement with those obtained by Remscheid *et al.* They have calculated the two lowest electronic states of the $N_2^{4+}$ transient molecular ion, namely the $^5\Sigma_u^+$ ground state and the $^3\Sigma_g^-$ state. Although the major component in the KER spectra of $N^{2+}$-$N^{2+}$ obtained in our experiment comes from the dissociation of the $^5\Sigma$ ground state of $N_2^{4+}$ into $N^{2+}(^4P)$ and $N^{2+}(^2D)$, there is also a high-energy component, part of which could be the contribution from the $^3\Sigma$ state of $N_2^{4+}$ dissociating into two ground states $N^{2+}(^2P)$. The dissociation energy for $N_2^{6+}$ as calculated by Remscheid *et al.* agrees with our experimental as well as our theoretically calculated values.

Safvan and Mathur [32] have also theoretically investigated the dissociation of highly charged $N_2^{q+}$ ($q \geqslant 2$) ions via non-Coulombic potential-energy curves. Some of the dissociation channels shown by them are multiplicity-forbidden and would result in KER values lower than predicted by them. In general, our theoretical values are in agreement with the values obtained by them.

From the comparative yield of the two ion pairs that correspond to different dissociation channels of a single parent molecular ion, we find that the symmetric breakup is preferred over asymmetric, in agreement with the experimental observations of Ref. [31]. From the comparisons of the KER distributions of such ion pairs, we observe that for the asymmetric charge dissociation channel there are two energy components in the KER distribution while the charge symmetric channel has a single peak for the most probable KER. Also, in the case of $N_2^{4+}$ and $N_2^{6+}$ breakup, the two possible channels (symmetric breakup and asymmetric breakup) show different energy components. This implies that the states leading to the symmetric and the asymmetric breakup are independent of each other.

At the projectile velocity range used in the present experiment, transfer ionization is the dominant process of electron transfer [20] and thus there is a possibility of the target being left in an excited state after the ion-molecule interaction. The excited particle then relaxes to the ground state either by Auger emission or radiative decay. The Auger emission lifetimes are of the same order as the characteristic fragmentation time of the molecules and hence only an energy analysis of the emitted electrons in the case of ion-molecule collisions can explain the origin of the emitted electrons. Target excitation following ion impact has been observed to play a significant role in multielectron capture studies in ion-atom collision experiments [33]. Not many reports exist to comment on the role of target excitation in ion-molecule collisions. Lablanquie *et al.* [34] had reported the possibility of autoionization in $CO^+$ leading to production of $C^+$ and $O^+$ ions with low kinetic energy releases. A later study [35] using high- and low-energy projectiles interacting with CO, however, indicated that target excitation does not seem to take place. The occurrence of a low-energy peak at 72 eV in the $N^{3+}$-$N^{3+}$ fragmentation channel is strong evidence of core excitation of $N_2$ during ion impact as this peak can only be explained by the Auger emission of $N^{2+}$ formed during the dissociation of $N_2^{5+}$ into $N^{2+}$ and $N^{3+}$. It is worth noting that the relative cross section for production of the $N^{3+}$-$N^{3+}$ ion pair following Auger emission is much greater than its production following decay of the $N_2^{6+}$ transient molecular ion. This implies that the probability of direct ionization of six electrons is less than the probabilty of five-electron ionization accompanied by core excitation.

## V. CONCLUSION

We have presented the results of a study of ion-induced fragmentation of $N_2$ using time-of-flight coincidence techniques. The time and position data obtained during the experiment were analyzed on an event-by-event basis to determine the KER spectra corresponding to the various observed fragmentation channels. The KER spectra are explained on the basis of existing and calculated *ab initio* potential-energy curves of the molecular $N_2^{q+}$ ions with ($3 \leqslant q \leqslant 6$). Good agreement is found between the theoretically calculated and experimentally determined KER values. The high-energy component in almost all the KER spectra is originating from the population of the excited intermediate molecular states resulting in the formation of low-lying atomic fragments. We have found a signature of core excitation of the target molecule following ion impact in the form of a clear distinct peak at 72 eV in the $N^{3+}$-$N^{3+}$ KER spectra having an energy close to the probable KER in the case of the $N^{2+}$-$N^{3+}$ fragmentation channel. The origin of this peak lies in the Auger emission of the $N^{2+}$ ion formed during the dissociation of the $N_2^{5+}$ transient molecular ion into $N^{2+}$ and $N^{3+}$. Further studies measuring the energy of the emitted electrons are needed to verify the origin of the electrons and identify the role of target excitation in ion-molecule collisions.

**ACKNOWLEDGMENTS**

The authors wish to acknowledge the support of LEIBF staff for the successful completion of this experiment. J.R. thanks the Council for Scientific and Industrial Research (CSIR), India and S.D. thanks the University Grants Comission (UGC), India for providing financial support.

[1] S. W. J. Scully, J. A. Wyer, V. Senthil, M. B. Shah, and E. C. Montenegro, Phys. Rev. A **73**, 040701(R) (2006).
[2] P. Baltzer, M. Lundqvist, B. Wannberg, L. Karlsson, M. Larsson, M. A. Hayes, J. B. West, M. R. F. Siggel, A. C. Parr, and J. L. Dehmer, J. Phys. B **27**, 4915 (1994).
[3] F. A. Rajgara, M. Krishnamurthy, and D. Mathur, Phys. Rev. A **68**, 023407 (2003).
[4] B. Seigmann, U. Werner, and H. Lutz, Aust. J. Phys. **52**, 545 (1999).
[5] M. Ehrich, B. Seigmann, U. Werner, and H. Lebius, Radiat. Phys. Chem. **68**, 127 (2003).
[6] H. O. Folkerts, R. Hoekstra, and R. Morgenstern, Phys. Rev. Lett. **77**, 3339 (1996).
[7] F. A. Rajgara, M. Krishnamurthy, D. Mathur, T. Nishide, T. Kitamura, H. Shiromaru, Y. Achiba, and N. Kobayashi, Phys. Rev. A **64**, 032712 (2001).
[8] B. Siegmann, U. Werner, R. Mann, N. M. Kabachnik, and H. O. Lutz, Phys. Rev. A **62**, 022718 (2000).
[9] D. Mathur, E. Krishnakumar, K. Nagesha, V. R. Marathe, V. Krishnamurthi, F. A. Rajgara, and U. T. Raheja, J. Phys. B **26**, L141 (1993).
[10] M. Tarisien *et al.*, J. Phys. B **33**, L11 (2000).
[11] R. D. DuBois, T. Schlatholter, O. Hadjar, R. Hoekstra, R. Morgenstern, C. M. Doudna, R. Feeler, and R. E. Olson, Europhys. Lett. **49**, 41 (2000).
[12] T. Kaneyasu, K. Matsuda, M. Ehrich, M. Yoshino, and K. Okuno, Phys. Scr., T **T92**, 341 (2001).
[13] W. Eberhardt, T. K. Sham, R. Carr, S. Krummacher, M. Strongin, S. L. Weng, and D. Wesner, Phys. Rev. Lett. **50**, 1038 (1983).
[14] W. Eberhardt, J. Stöhr, J. Feldhaus, E. W. Plummer, and F. Sette, Phys. Rev. Lett. **51**, 2370 (1983).
[15] W. Eberhardt, E. W. Plummer, I. W. Lyo, R. Carr, and W. K. Ford, Phys. Rev. Lett. **58**, 207 (1987).
[16] M. Neeb, A. Kivimäki, B. Kempgens, H. M. Köppe, J. Feldhaus, and A. M. Bradshaw, Phys. Rev. Lett. **76**, 2250 (1996).
[17] J.-E. Rubensson, J. Lüning, M. Neeb, B. Küpper, S. Eisebitt, and W. Eberhardt, Phys. Rev. Lett. **76**, 3919 (1996).
[18] R. G. Hayes and W. Eberhardt, J. Chem. Phys. **94**, 6398 (1991).
[19] F. Alvarado, R. Hoekstra, and T. Schlathölter, J. Phys. B **38**, 4085 (2005).
[20] W. Groh, A. Muller, A. S. Schlachter, and E. Salzborn, J. Phys. B **16**, 1997 (1983).
[21] D. Kanjilal, T. Madhu, G. O. Rodrigues, U. Rao, C. P. Safvan, and A. Roy, Indian J. Pure Appl. Phys. **39**, 25 (2001).
[22] S. De, P. N. Ghosh, A. Roy, and C. P. Safvan, Nucl. Instrum. Methods Phys. Res. B **243**, 435 (2006).
[23] M. W. Schmidt *et al.*, J. Comput. Chem. **14**, 1347 (1993).
[24] http://www.nist.gov/srd/.
[25] R. W. Wetmore and R. K. Boyd, J. Phys. Chem. **90**, 5540 (1986).
[26] M. Lundqvist, D. Edvardsson, P. Baltzer, and B. Wannberg, J. Phys. B **29**, 1489 (1996).
[27] A. D. Bandrauk, D. G. Musaev, and K. Morokuma, Phys. Rev. A **59**, 4309 (1999).
[28] C. J. Latimer, Adv. At., Mol., Opt. Phys. **30**, 105 (1993).
[29] I. Ben-Itzhak, S. G. Ginther, V. Krishnamurthi, and K. D. Carnes, Phys. Rev. A **51**, 391 (1995).
[30] U. Brikmann, A. Reinkoster, B. Siegmann, U. Werner, H. O. Lutz, and R. Mann, Phys. Scr., T **T80**, 171 (1999).
[31] A. Remscheid, B. A. Huber, M. Pykavyj, V. Staemmler, and K. Wiesemann, J. Phys. B **29**, 515 (1996).
[32] C. P. Safvan and D. Mathur, J. Phys. B **27**, 4073 (1994).
[33] A. A. Hasan, E. D. Emmons, G. Hinojosa, and R. Ali, Phys. Rev. Lett. **83**, 4522 (1999).
[34] P. Lablanquie *et al.*, Phys. Rev. A **40**, 5673 (1989).
[35] M. Tarisien *et al.*, J. Phys. B **33**, L11 (2000).